Article ID: 1006-8775(2009) 01-0148-08

DOMINANT PHYSICAL PROCESSES ASSOCIATED WITH PHASE DIFFERENCES BETWEEN SURFACE RAINFALL AND CONVECTIVE AVAILABLE POTENTIAL ENERGY

Xiaofan LI (李小凡)

(NOAA/NESDIS/Center for Satellite Applications and Research Camp Springs, Maryland, USA)

Abstract: A lag correlation analysis is conducted with a 21-day TOGA COARE cloud-resolving model simulation data to identify the phase relation between surface rainfall and convective available potential energy (CAPE) and associated physical processes. The analysis shows that the maximum negative lag correlations between the model domain mean CAPE and rainfall occurs around lag hour 6. The minimum mean CAPE lags mean and convective rainfall through the vapor condensation and depositions, water vapor convergence, and heat divergence whereas it lags stratiform rainfall via the transport of hydrometeor concentration from convective regions to raining stratiform regions, vapor condensation and depositions, water vapor storage, and heat divergence over raining stratiform regions.

Key words: phase relation; convective available potential energy; surface rainfall; cloud-resolving model simulation

CLC number: P426.61 **Document code:** A **doi:** 10.3969/j.issn.1006-8775.2009.02.003

1 INTRODUCTION

Surface rainfall is a result of release of unstable energy during convective development. The buildup of unstable energy usually occurs in favorable environmental thermodynamic conditions when the rainfall is absent. The release of unstable energy triggered by large-scale circulation, topography, and interactions with other weather systems leads to the growth of cloud systems, with the aid of water vapor transport, and thus the torrential rainfall. The torrential rainfall is usually associated with strong weather systems such as tropical cyclones (tropical storms and typhoons in tropical western Pacific). The buildup of unstable energy and rainfall cannot occur simultaneously. The phase relation between the unstable energy and surface rainfall is an important issue in developing cumulus parameterization schemes[1-3]. Xu and Randall[4] analyzed two-dimensional (2D) cloud-resolving model simulations, demonstrated that the minimum convective available potential energy (CAPE) lags the rainfall peak by a few hours, and argued that the phase lag is the adjustment time scale from disequilibrium to equilibrium states in the presence of temporally-varying large-scale forcing. Li et al.[5] examined budgets of mean moist available potential energy and perturbation kinetic energy that represent CAPE and surface rainfall, respectively, and conducted process study associated with the phase lag between mean moist available potential energy and perturbation kinetic energy.

Recently, Gao et al.[6] and Gao and Li [7] derived a set of surface rainfall equations by combining water vapor and heat budgets with cloud budget. The direct linkage of water vapor, heat, and cloud processes to surface rainfall allows us to directly revisit the phase difference between CAPE and surface rainfall, without the aid of energy analysis. In this study, a lag correlation analysis between CAPE and surface rainfall is conducted using a 2D cloud-resolving model experiment that is forced by the large-scale forcing derived from Tropical Ocean Global Atmosphere Coupled Ocean-Atmosphere Response Experiment (TOGA COARE). In the next section, the cloud model, forcing, and experiment are described. The results are presented in section 3. The summary is given in section 4.

2 MODEL AND EXPERIMENT

Received date: 2009-03-28; **revised date:** 2009-09-01

Biography: Xiaofan LI, PhD, undertaking the research on cloud resolving modeling, ocean modeling, geophysical fluid dynamics.

E-mail for correspondence author: xiaofan.li@noaa.gov

The data analyzed in this study is from the 2D cloud-resolving model simulation conducted by Li et al.[8]. The model is forced by zonally-uniform vertical velocity, zonal wind, and thermal and moisture advection based on 6-hourly TOGA COARE observations within the Intensive Flux Array (IFA) region and hourly sea surface temperature (SST) at the Improved Meteorological (IMET) surface mooring buoy (1.75°S, 156°E)[9] (Fig. 1). The model is integrated from 0400 LST 18 December 1992 to 1000 LST 9 January 1993 (A total of 486 hours). The model simulation data have been used to study surface rainfall processes[6, 7, 10-12], precipitation efficiency[8, 13, 14], convective, moist, and dynamic vorticity vector[15, 16], effects of ice clouds on rainfall[17], rainfall responses to large-scale forcing [18, 19], cloud clusters and merging[20], diurnal variations of tropical oceanic rainfall [21], and convective and stratiform rainfall and partitioning [22-24].

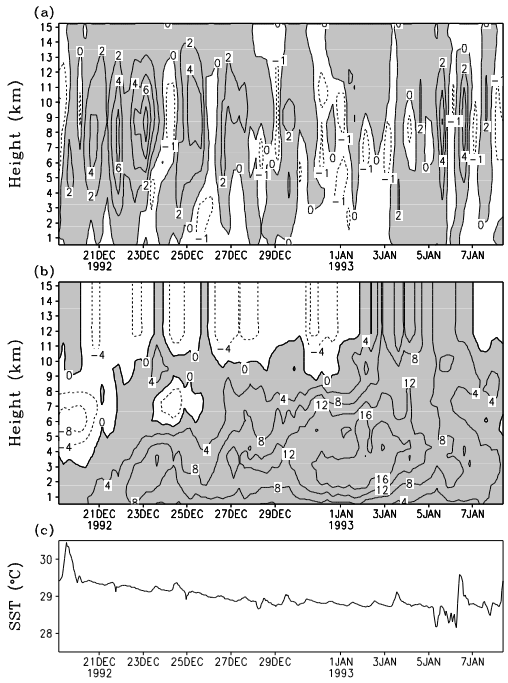

Fig.1 Time-height cross sections of (a) vertical velocity (cm s^{-1}), (b) zonal wind (m s^{-1}), and time series of (c) sea surface temperature (°C) observed and derived from TOGA COARE for the 21-day period. Upward motions in (a) and westerly winds in (b) are shaded.

The cloud resolving model used in the paper has prognostic equations of potential temperature, specific humidity, mixing ratios of cloud water, raindrop, cloud ice, snow, and graupel, and perturbation momentum. The model also includes the cloud microphysical parameterization schemes, and interactive solar and thermal infrared radiation parameterization schemes. The model uses cyclic lateral boundaries, and a horizontal domain of 968 km, a horizontal grid resolution of 1.5 km, 33 vertical levels, and a time step of 12 s. The detailed descriptions of the model can be found in Gao and Li[25]. The validated model simulation data have been analyzed for process studies such as effects of vertical wind shear[26] and cloud radiative processes[27] on rainfall of Tropical Storm Bilis (2006), sensitivities of cloud and rainfall simulations to uncertainties of initial conditions[28-31], tropical climate equilibrium states[32-35], and diurnal variations of tropical convective and stratiform rainfall [36, 37].

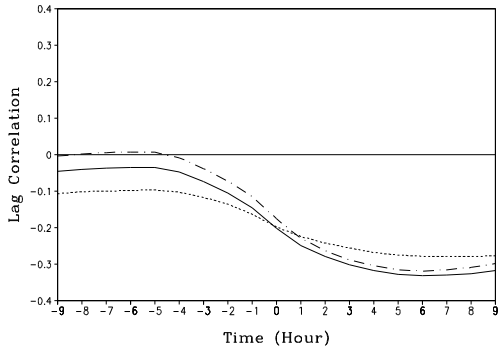

Fig.2 Lag correlation between model domain mean CAPE and mean surface rain rate (solid), mean CAPE and stratiform rain rate (dash), and mean CAPE and convective rain rate (dot dash).

3 RESULTS

The phase difference between surface rainfall (P_S) and convective available potential energy (CAPE) is examined by calculating lag correlation coefficients between P_S and CAPE. Positive lag hour denote CAPE lags P_S and negative correlation means correlation of minimum CAPE with maximum P_S. Figure 2 shows that minimum model domain mean CAPE lags maximum P_S by about 6 hours. This indicates that the maximum release of CAPE is responsible for the rainfall peak. The CAPE is calculated under reversible moist adiabatic process[5]. The lag correction is –0.33. A Student's *t*-test on the significance of the lag correlation coefficients is further conducted using 474 degrees of freedom and a critical correlation coefficient at the 1% significant level is 0.13. Thus, the lag correlation of maximum mean surface rainfall by minimum mean CAPE is statistically significant.

The mean surface rainfall consists of stratiform

and convective rainfall. The convective-stratiform rainfall partitioning scheme used in this study is developed by Tao et al.[38] and modified by Sui et al.[39]. This scheme separates each vertical column containing clouds in a 2D *x*-*z* framework into convective or stratiform based on the following criterion. Model grid point is identified as convective if it has a rain rate twice as large as the average taken over the surrounding four grid points, the one grid point on either side of this grid point, and any grid point with a rain rate of 20 mm h^{-1} or more. All non-convective cloudy points are considered as stratiform. In addition, grid points in the stratiform region are further checked and identified as convective when the following conditions are met. In the raining stratiform region, cloud water below the melting level is greater than 0.5 g kg^{-1} or the maximum updraft above 600 hPa exceeds 5 m s^{-1}, or in the non-raining stratiform region, cloud water of 0.025 g kg^{-1} or more exists or the maximum updraft exceeds 5 m s^{-1} below the melting level. The minimum mean CAPE lags maximum stratiform rainfall by 7 hours with the maximum negative correlation of –0.28, whereas it lags maximum convective rainfall by 6 hours with the maximum negative correlation of –0.32. Both are above the 1% significant level.

To examine dominant rainfall processes that are responsible for the phase differences between CAPE and surface rainfall, surface rainfall budgets are analyzed. The surface rainfall equation can be written in cloud budget, which is expressed by

$$P_S = Q_{WVOUT} + Q_{WVIN} + Q_{CM}, \tag{1}$$

where

$$Q_{CM} = -\frac{\partial [q_l]}{\partial t} - [u\frac{\partial q_l}{\partial x}] - [w\frac{\partial q_l}{\partial z}], \tag{1a}$$

$$Q_{WVOUT} = [P_{CND}] + [P_{DEP}] + [P_{SDEP}] + [P_{GDEP}], \tag{1b}$$

$$Q_{WVIN} = -[P_{REVP}] - [P_{MLTG}] - [P_{MLTS}]. \tag{1c}$$

Here, P_S is surface rain rate; u and w are zonal and vertical wind components, respectively; $q_l = q_c + q_r + q_i + q_s + q_g$, q_c, q_r, q_i, q_s, q_g are the mixing ratios of cloud water, raindrops, cloud ice, snow, and graupel, respectively; $[()] = \int_{z_b}^{z_t} \overline{\rho}()dz$, z_t and z_b are the heights of the top and bottom of the model atmosphere respectively; the cloud microphysical processes in Eqs. (1b) and (1c) can be found in Table 1. In cloud budget, surface rainfall is determined by vapor condensation and deposition (Q_{WVOUT}), evaporation of precipitation hydrometeor (Q_{WVIN}), and hydrometeor storage minus convergence (Q_{CM}). The surface rainfall equation can be derived by combining water vapor budget with cloud budget as proposed by Gao et al.[6], which is written as

$$P_S = Q_{WVT} + Q_{WVF} + Q_{WVE} + Q_{CM}, \tag{2}$$

where

$$Q_{WVT} = -\frac{\partial [q_v]}{\partial t}, \tag{2a}$$

$$Q_{WVF} = -[\overline{u}^o \frac{\partial \overline{q}_v}{\partial x}] - [\overline{w}^o \frac{\partial \overline{q}_v}{\partial z}] - [\frac{\partial (u' q_v')}{\partial x}] - [\overline{u}^o \frac{\partial q_v'}{\partial x}] - [\overline{w}^o \frac{\partial q_v'}{\partial z}] - [w' \frac{\partial \overline{q}_v'}{\partial z}], \tag{2b}$$

$$Q_{WVE} = E_s \tag{2c}$$

Here, q_v is specific humidity; E_s is surface evaporation; the overbar denotes a model domain mean; the prime is a perturbation from model domain mean; and the superscript "o" is an imposed COARE-observed value. The surface rainfall is determined by water vapor storage (Q_{WVT}), water vapor convergence (Q_{WVF}), surface evaporation (Q_{WVE}), and hydrometeor storage minus convergence (Q_{CM}) in the surface rainfall equation derived from cloud and water vapor budgets. The surface rainfall equation can be derived by combining heat budget with cloud budget as proposed by Gao and Li[7], which is written as

$$P_S = S_{HT} + S_{HF} + S_{HS} + S_{LHLF} + S_{RAD} + Q_{CM}, \tag{3}$$

where

$$S_{HT} = \frac{c_p}{L_v}\frac{\partial [T]}{\partial t}, \tag{3a}$$

$$S_{HF} = \frac{c_p}{L_v}[\frac{\partial}{\partial x}(\overline{u}^o + u')T' + \pi \overline{u}^o \frac{\partial \overline{\theta}^o}{\partial x} + \pi \overline{w}^o \frac{\partial}{\partial z}(\overline{\theta} + \theta') + \pi w' \frac{\partial \overline{\theta}}{\partial z}], \tag{3b}$$

$$S_{HS} = -\frac{c_p}{L_v} H_s, \tag{3c}$$

$$S_{LHLF} = -\frac{L_f}{L_v} < P_{18} >, \tag{3d}$$

$$S_{RAD} = -\frac{1}{L_v} < Q_R >, \tag{3e}$$

$$P_{18} = P_{DEP} + P_{SDEP} + P_{GDEP} - P_{MLTS} - P_{MLTG} + P_{SACW}(T < T_o) + P_{SFW}(T < T_o) + P_{GACW}(T < T_o) + P_{IACR}(T < T_o) + P_{GACR}(T < T_o) + P_{SACR}(T < T_o) + P_{GFR}(T < T_o) - P_{RACS}(T > T_o) - P_{SMLT}(T > T_o)$$

$$-P_{GMLT}(T>T_o)+P_{IHOM}(T<T_{oo})-P_{IMLT}(T>T_o)+P_{IDW}(T_{oo}<T<T_o), \quad (3f)$$

where T and θ are temperature and potential temperature, respectively; H_s is surface sensible heat flux; c_p is the specific heat of dry air at constant pressure; L_v, L_s, and L_f are latent heat of vaporization, sublimation, and fusion at T_o=0°C, respectively, L_s=L_v+L_f; T_{oo} = –35°C; and cloud microphysical processes in Eq. (3g) can be found in Table 1. Q_R is the radiative heating rate due to the convergence of net flux of solar and infrared radiative fluxes. The surface rainfall is determined by heat storage (S_{HT}), heat divergence (S_{HF}), surface sensible heat (S_{HS}), latent heat associated with ice microphysical processes (S_{LHLF}), and radiative heating (S_{RAD}).

To elucidate the dominant rainfall processes that are responsible for the maximum negative lag correlation coefficients between mean CAPE and surface rainfall, the lag correlation coefficient can be expanded into

$$C_{CAPE,P_S}=\sum_{i=1}^{n}\frac{\sigma_{P_{Si}}}{\sigma_{P_S}}C_{CAPE,P_{Si}} \quad (4)$$

where σ is a standard deviation and $\frac{\sigma_{P_{Si}}}{\sigma_{P_S}}C_{CAPE,P_S}$ is a weighted lag correlation coefficient between CAPE and P_S. In Eq. (4), n=3, P_S =(Q_{WVOUT}, Q_{WVIN}, Q_{CM}) for lag correlation of CAPE with Eq. (1), n=4, P_S =(Q_{WVT}, Q_{WVF}, Q_{WVE}, Q_{CM}) for lag correlation of CAPE with Eq. (2), and n=6, P_S =(S_{HT}, S_{HF}, S_{HS}, S_{LHLF}, S_{RAD}, Q_{CM}) for lag correlation of CAPE with Eq. (3).

The maximum negative lag correlation of mean CAPE with mean surface rainfall is determined by the maximum negative lag correlation of mean CAPE with mean Q_{WVOUT} (–0.47 at lag hour 6) (Fig. 3a) when the surface rainfall is accounted for by cloud microphysical processes in Eq. (1). When the surface rainfall is accounted for by the water vapor budget in Eq. (2) and by the heat budget in Eq. (3), only the lag correlations between mean CAPE and mean Q_{WVF} and between mean CAPE and mean S_{HF} are statistically significant (Fig. 3b & 3c). The negative lag correlation coefficients increase their magnitudes with increasing lag hours (~ –0.3 at lag hour 9), which are mainly responsible for the lag of maximum mean surface rainfall by minimum mean CAPE. The mean Q_{WVT} also lags mean P_S by 3 hours, and mean S_{HT} lags mean P_S by 2 hours. The correlation coefficients are about –0.1, which are below the 1% level of significance. However, Q_{WVT} and S_{HT} are as important as Q_{WVF} in regulating the lag hours between CAPE and P_S.

Table 1 List of microphysical processes and parameterization schemes from RH83[42], RH84[43], LFO[44], TSM[45], and KFLC[46].

Notation	Description	Scheme
P_{MLTG}	Growth of vapor by evaporation of liquid from graupel surface	RH84
P_{MLTS}	Growth of vapor by evaporation of melting snow	RH83
P_{REVP}	Growth of vapor by evaporation of raindrops	RH83
P_{IMLT}	Growth of cloud water by melting of cloud ice	RH83
P_{CND}	Growth of cloud water by condensation of supersaturated vapor	TSM
P_{GMLT}	Growth of raindrops by melting of graupel	RH84
P_{SMLT}	Growth of raindrops by melting of snow	RH83
P_{RACI}	Growth of raindrops by the accretion of cloud ice	RH84
P_{RACW}	Growth of raindrops by the collection of cloud water	RH83
P_{RACS}	Growth of raindrops by the accretion of snow	RH84
P_{RAUT}	Growth of raindrops by the autoconversion of cloud water	LFO
P_{IDW}	Growth of cloud ice by the deposition of cloud water	KFLC
P_{IACR}	Growth of cloud ice by the accretion of rain	RH84
P_{IHOM}	Growth of cloud ice by the homogeneous freezing of cloud water	
P_{DEP}	Growth of cloud ice by the deposition of supersaturated vapor	TSM
P_{SAUT}	Growth of snow by the conversion of cloud ice	RH83
P_{SACI}	Growth of snow by the collection of cloud ice	RH83
P_{SACW}	Growth of snow by the accretion of cloud water	RH83
P_{SFW}	Growth of snow by the deposition of cloud water	KFLC
P_{SFI}	Depositional growth of snow from cloud ice	KFLC
P_{SACR}	Growth of snow by the accretion of raindrops	LFO
P_{SDEP}	Growth of snow by the deposition of vapor	RH83
P_{GACI}	Growth of graupel by the collection of cloud ice	RH84
P_{GACR}	Growth of graupel by the accretion of raindrops	RH84
P_{GACS}	Growth of graupel by the accretion of snow	RH84
P_{GACW}	Growth of graupel by the accretion of cloud water	RH84
P_{WACS}	Growth of graupel by the riming of snow	RH84
PGDEP	Growth of graupel by the deposition of vapor	RH84
PGFR	Growth of graupel by the freezing of raindrops	LFO

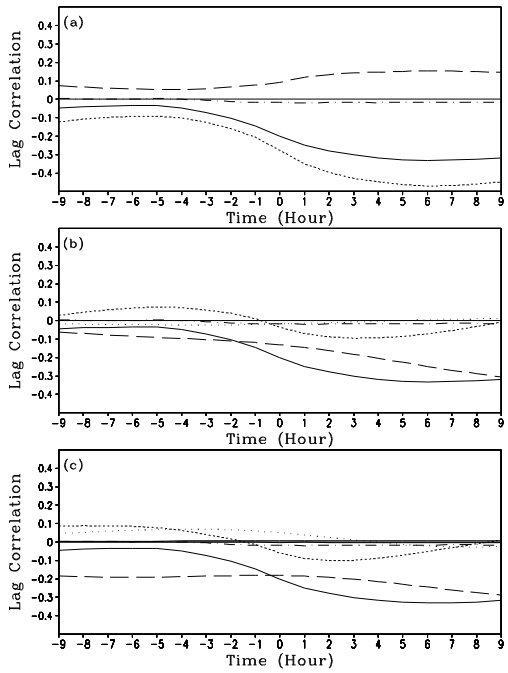

Fig.3 Lag correlations of model domain mean CAPE with means of P_S (solid), Q_{WVOUT} (dash), Q_{WVIN} (long dash), and Q_{CM} (dot dash) in (a), P_S (solid), Q_{WVT} (dash), Q_{WVF} (long dash), Q_{WVE} (dot), and Q_{CM} (dot dash) in (b), and P_S (solid), S_{HT} (dash), S_{HF} (long dash), S_{RAD} (dot), and Q_{CM} (dot dash) in (c). Lag correlations of model domain mean CAPE with means of S_{HS} and S_{LHLF} are presented in (c) because they are negligibly small.

The maximum negative lag correlation of mean CAPE with stratiform rainfall is determined by the maximum negative lag correlations of mean CAPE with the components of Q_{WVOUT} (–0.37 at lag hour 9) and Q_{CM} (–0.16 at lag hour 6) in Eq. (1) (Fig. 4a), with the components of Q_{WVT} (–0.15 at lag hour 9) and Q_{CM} (–0.16 at lag hour 6) in Eq. (2) (Fig. 4b), and with the components of S_{HF} (–0.15 at lag hour 9) and Q_{CM} (–0.16 at lag hour 6) in Eq. (3) (Fig. 4c) over raining stratiform regions. This indicates that the vapor condensation and deposition, water vapor storage, heat divergence, and transport of hydrometeor concentration from convective regions to raining stratiform regions are responsible for the lag of mean CAPE with stratiform rainfall. The important roles the transport of hydrometeor concentration from convective regions to raining stratiform regions plays in the phase relation between unstable energy and stratiform rainfall are consistent with the water budget analysis of tropical and midlatitude convective systems [20, 40, 41]. The water vapor storage and heat divergence are crucial in determining the phase relation, suggesting different dominant rainfall processes associated with stratiform rainfall. The maximum negative lag correlation of mean CAPE with convective rainfall is determined by the maximum negative lag correlations of mean CAPE with the component of Q_{WVOUT} (–0.43 at lag hour 6) in Eq. (1) (Fig. 5a), with the component of Q_{WVF} (–0.43 at lag hour 6) in Eq. (2) (Fig. 5b), and with the component of S_{HF} (–0.37 at lag hour 6) in Eq. (3) (Fig. 5c). This suggests that the vapor condensation and deposition, water vapor convergence, and heat divergence mainly account for the lag of mean CAPE with convective rainfall. The important roles water vapor convergence and heat divergence play in determining the phase relation between mean CAPE and convective rainfall imply dominant updraft in water vapor and heat budget during convective development.

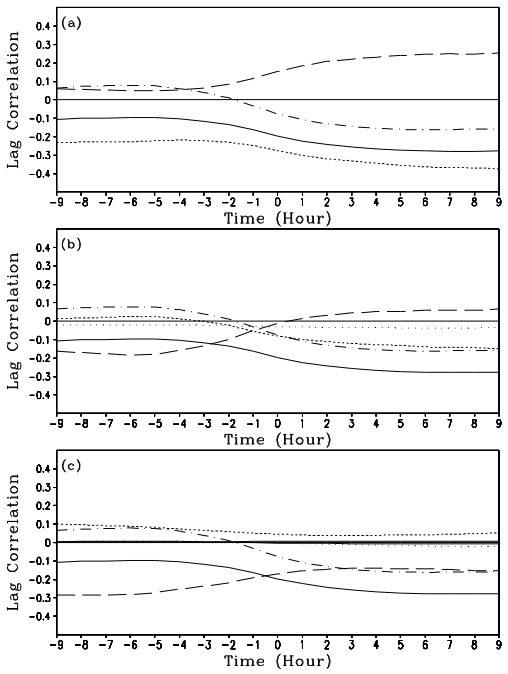

Fig.4 Lag correlations of model domain mean CAPE with raining stratiform components of P_S (solid), Q_{WVOUT} (dash), Q_{WVIN} (long dash), and Q_{CM} (dot dash) in (a), P_S (solid), Q_{WVT} (dash), Q_{WVF} (long dash), Q_{WVE} (dot), and Q_{CM} (dot dash) in (b), and P_S (solid), S_{HT} (dash), S_{HF} (long dash), S_{RAD} (dot), and Q_{CM} (dot dash) in (c). Lag correlations of model domain mean CAPE with means of S_{HS} and S_{LHLF} are presented in (c) because they are negligibly small.

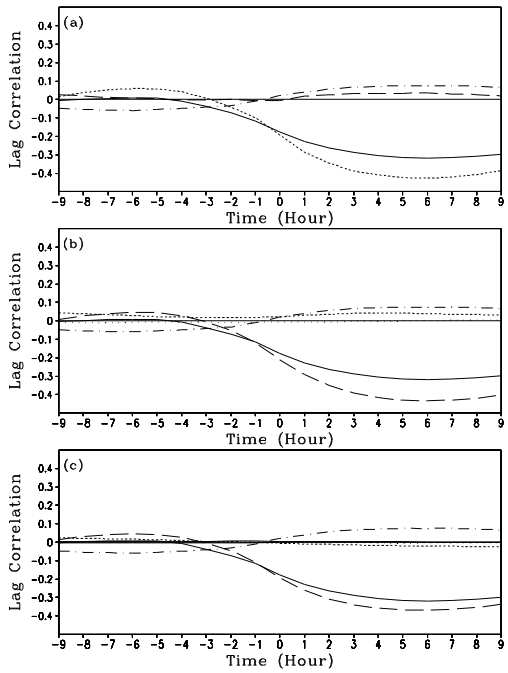

Fig.5 Lag correlations of model domain mean CAPE with convective components of P_S (solid), Q_{WVOUT} (dash), Q_{WVIN} (long dash), and Q_{CM} (dot dash) in (a), P_S (solid), Q_{WVT} (dash), Q_{WVF} (long dash), Q_{WVE} (dot), and Q_{CM} (dot dash) in (b), and P_S (solid), S_{HT} (dash), S_{HF} (long dash), S_{RAD} (dot), and Q_{CM} (dot dash) in (c). Lag correlations of model domain mean *CAPE* with means of S_{HS} and S_{LHLF} are presented in (c) because they are negligibly small.

4 SUMMARY

The dominant physical processes responsible for the phase relation between surface rainfall and convective available potential energy (CAPE) are examined by conducting a lag correlation analysis on cloud-resolving model simulation. The model is integrated for 21 days with the large-scale forcing from TOGA COARE. The maximum negative lag correlations between the model domain mean CAPE and surface rainfall occur around lag hour 6, showing that the minimum mean CAPE lags maximum mean, convective, and stratiform rainfall by about 6 hours. The major processes that control the phase lag of the minimum mean CAPE from the mean rainfall peak are the mean vapor condensation and depositions, mean water vapor convergence, and mean heat divergence. The water vapor and heat storage are important in determining lag hour, although their lag correlations with the mean CAPE are not statistically significant. Since the mean water vapor convergence and heat divergence are mainly associated with imposed large-scale vertical velocity, the imposed large-scale forcing plays a crucial role in determining the maximum negative lag correlation. The transport of hydrometeor concentration from convective regions to raining stratiform regions, vapor condensation and depositions, water vapor storage, and heat divergence over raining stratiform regions are mainly responsible for the maximum negative lag correlation between the mean CAPE and stratiform rainfall. The vapor condensation and depositions, water vapor convergence, and heat divergence over convective regions mainly account for the maximum negative lag correlation between the mean CAPE and convective rainfall.

***Acknowledgement*:** The author thanks Dr. W.-K. Tao, NASA/GSFC, USA, for his two-dimensional cloud resolving model, and Prof. M. Zhang, the State University of New York at Stony Brook, USA, for his TOGA COARE forcing data.

REFERENCES:

[1] ARAKAWA A, SCHUBERT W H. Interaction of a cumulus cloud ensemble with the large-scale environment. Part I [J]. J. Atmos. Sci., 1974, 31: 674-701.
[2] BETTS A K, MILLER M J. A new convective adjustment scheme. Part II: Single column tests using GATE wave, BOMEX, ATEX and Artic airmass data set [J]. Quart. J. Roy. Meteor. Soc., 1986, 112: 692-709.
[3] RANDALL D A, PAN D M. Implementation of the Arakawa-Schubert cumulus parameterization with a prognostic closure. [J]. Meteor. Monogr., Amer. Meteor. Soc., 1993, 46: 137-144.
[4] XU K M, RANDALL D A. Explicit simulation of cumulus ensembles with the GATE Phase III data: Comparison with observations [J]. J. Atmos. Sci., 1996, 53: 3710-3736.
[5] LI X, SUI C H, LAU K M. Interactions between tropical convection and its embedding environment: An energetics analysis of a 2-D cloud resolving simulation [J]. J. Atmos. Sci., 2002, 59: 1712-1722.
[6] GAO S, CUI X, ZHOU Y, et al. Surface rainfall processes as simulated in a cloud resolving model [J]. J. Geophys. Res., 2005, 110, D10202, doi: 10.1029/2004JD005467.
[7] GAO S, LI X. Precipitation equations and their applications to the analysis of diurnal variation of tropical oceanic rainfall [J]. J. Geophys. Res., 2009, revised.
[8] LI X, SUI C H, LAU K M. Precipitation efficiency in the tropical deep convective regime: A 2-D cloud resolving modeling study [J]. J. Meteor. Soc. Japan, 2002, 80: 205-212.
[9] WELLER R A, ANDERSON S P. Surface meteorology and air-sea fluxes in the western equatorial Pacific warm pool during TOGA COARE [J]. J. Climate, 1996, 9: 1959-1990.
[10] LI X, SUI C H, LAU K M. Dominant cloud microphysical processes in a tropical oceanic convective system: A 2-D cloud resolving modeling study [J]. Mon. Wea. Rev. 2002, 130: 2481-2491.
[11] ZHOU Y, CUI X, LI X. Contribution of cloud condensate to Surface rain rate [J]. Prog. Nat. Sci., 2006, 16: 967-973.
[12] CUI X, LI X. Role of surface evaporation in surface rainfall processes [J]. J. Geophys. Res. 2006, 111, D17112, doi: 10.1029/2005JD006876.
[13] SUI C H, Li X, YANG M J, et al. Estimation of oceanic precipitation efficiency in cloud models [J]. J. Atmos. Sci., 2005, 62: 4358-4370.

[14] SUI C H, LI X, YANG M J. On the definition of precipitation efficiency [J]. J. Atmos. Sci., 2007, 64: 4506-4513.
[15] GAO S, PING F, LI X, et al. A convective vorticity vector associated with tropical convection: A 2D cloud-resolving modeling study [J]. J. Geophys. Res., 2004, 109, D14106, doi: 10.1029/2004JD004807.
[16] GAO S, CUI X, ZHOU Y, et al. A modeling study of moist and dynamic vorticity vectors associated with 2D tropical convection [J]. J. Geophys. Res., 2005, 110, D17104, doi: 10.1029/2004JD005675.
[17] GAO S, RAN L, LI X. Impacts of ice microphysics on rainfall and thermodynamic processes in the tropical deep convective regime: A 2D cloud-resolving modeling study [J]. Mon. Wea. Rev., 2006, 134: 3015-3024.
[18] GAO S, Ping F, Li X. Tropical heat/water quasi-equilibrium and cycle as simulated in a 2D cloud resolving model [J]. Atmos. Res., 2006, 79:15-29.
[19] GAO S, LI X. Responses of tropical deep convective precipitation systems and their associated convective and stratiform regions to the large-scale forcing [J]. Quart. J. Roy. Meteor. Soc, 2008, 134: 2127-2141.
[20] PING F, LUO Z, LI X. Kinematics, Cloud microphysics, and spatial structures of tropical cloud clusters: A two-dimensional cloud-resolving modeling study [J]. Atmos. Res., 2008, 88: 323-336.
[21] GAO S, CUI X, LI X. A modeling study of diurnal rainfall variations during the 21-day period of TOGA COARE [J]. Adv. Atmos. Sci., 2009, 26: 895-905.
[22] SUI C H, LI X. A tendency of cloud ratio associated with the development of tropical water and ice clouds [J]. Terr. Atmos. Oceanic Sci., 2005, 16: 419-434.
[23] CUI X, ZHOU Y, LI X. Cloud microphysical properties in tropical convective and stratiform regions [J]. Meteor. Atmos. Phys., 2007, 98: 1-11.
[24] SUI C H, TSAY C T, LI X. Convective stratiform rainfall separation by cloud content [J]. J. Geophys. Res., 2007, 112, D14213, doi:10.1029/2006JD008082.
[25] GAO S, LI X. Cloud-resolving modeling of convective processes [M]. Dordrecht: Springer Press, 2008, 206 pp.
[26] WANG D, LI X, TAO W K, et al. Effects of vertical wind shear on convective development during a landfall of severe tropical storm Bilis (2006) [J]. Atmos. Res., 2009, 94: 270-275.
[27] WANG D, LI X, TAO W K. Cloud radiative effects on responses of convective and stratiform rainfall to large-scale forcing [J]. Atmos. Res., 2009, submitted.
[28] LI X, ZHANG S, ZHANG D L. Thermodynamic, cloud microphysics and rainfall responses to initial moisture perturbations in the tropical deep convective regime [J]. J. Geophys. Res., 2006, 111, D14207, doi:10.1029/2005JD006968.
[29] GAO S, LI X. Impacts of initial conditions on cloud-resolving simulations [J]. Adv. Atmos. Sci., 2008, 25: 737-747.
[30] GAO S, LI X. Dependence of the accuracy of precipitation and cloud simulation on time and spatial scales [J]. Adv. Atmos. Sci., 2009, in press.
[31] LI X, SHEN X. Sensitivity of cloud-resolving precipitation simulations to uncertainty of vertical structures of initial conditions [J]. Quart. J. Roy. Meteor. Soc., 2009, Revised.
[32] GAO S, ZHOU Y, LI X. Effects of diurnal variations on tropical equilibrium states: A two-dimensional cloud-resolving modeling study [J]. J. Atmos. Sci., 2007, 64: 656-664.
[33] GAO S. A cloud-resolving modeling study of cloud radiative effects on tropical equilibrium states [J]. J. Geophys. Res., 2008, 113, D03108, doi: 10.1029/2007JD009177.
[34] PING F, LUO Z, LI X. Microphysical and radiative effects of ice microphysics on tropical equilibrium states: A two-dimensional cloud-resolving modeling study [J]. Mon. Wea. Rev., 2007, 135: 2794-2802.
[35] ZHOU Y, Li X. Sensitivity of convective and stratiform rainfall to sea surface temperature [J]. Atmos. Res., 2009, 92: 212-219.
[36] CUI X. A cloud-resolving modeling study of diurnal variations of tropical convective and stratiform rainfall [J]. J. Geophys. Res., 2008, 113, D02113, doi: 10.1029/2007JD008990.
[37] CUI X, LI X. Diurnal responses of tropical convective and stratiform rainfall to diurnally varying sea surface temperature [J]. Meteor. Atmos. Phys., 2009, 104: 53-61.
[38] TAO W K, SIMPSON J, SUI C H, et al. Heating, moisture and water budgets of tropical and midlatitude squall lines: Comparisons and sensitivity to longwave radiation [J]. J. Atmos. Sci., 1993, 50: 673-690.
[39] SUI C H, LAU K M, TAO W K, et al. The tropical water and energy cycles in a cumulus ensemble model. Part I: Equilibrium climate [J]. J. Atmos. Sci., 1994, 51: 711-728.
[40] CHONG M, HAUSER D. A tropical squall line observed during the CORT 81 experiment in West Africa. Part II: Water budget [J]. Mon. Wea. Rev., 1989, 117: 728-744.
[41] GALLUS W A Jr., JOHNSON R H. Heat and moisture budgets of an intense midlatitude squall line [J]. J. Atmos. Sci., 1991, 48: 122-146.
[42] RUTLEDGE S A, Hobbs P V. The mesoscale and microscale structure and organization of clouds and precipitation in midlatitude cyclones. Part VIII: A model for the "seeder-feeder" process in warm-frontal rainbands [J]. J. Atmos. Sci., 1983, 40: 1185-1206.
[43] RUTLEDGE S A, HOBBS P V. The mesoscale and microscale structure and organization of clouds and precipitation in midlatitude cyclones. Part XII: A diagnostic modeling study of precipitation development in narrow cold-frontal rainbands [J]. J. Atmos. Sci., 1984, 41: 2949-2972.
[44] LIN Y L, FARLEY R D, ORVILLE H D. Bulk parameterization of the snow field in a cloud model [J]. J. Climate Appl. Meteor., 1983, 22: 1065-1092.
[45] TAO W K, SIMPSON J, McCUMBER M. An ice-water saturation adjustment [J]. Mon. Wea. Rev., 1989, 117: 231-235.
[46] KRUEGER S K, FU Q, LIOU K N, et al. Improvement of an ice-phase microphysics parameterization for use in numerical simulations of tropical convection [J]. J. Appl. Meteor., 1995, 34: 281-287.

Citation: Xiaofan LI. Dominant physical processes associated with phase differences between surface rainfall and convective available potential energy. *J. Trop. Meteor.*, 2009, 15(2): 148-154.